

STACKING APERTURES AND ESTIMATION STRATEGIES FOR REFLECTION AND DIFFRACTION ENHANCEMENT

J. H. Faccipieri Junior, T. A. Coimbra, L.-J. Gelius, and M. Tygel

email: *jorge.faccipieri@gmail.com, tgo.coimbra@gmail.com, l.j.gelius@geo.uio.no, tygel@ime.unicamp.br*

keywords: *Stacking apertures, Common Reflection Surface (CRS), Projected Fresnel Zone, Double Square Roots (DSR)*

ABSTRACT

It is well known that the quality of stacking results (e.g., noise reduction, event enhancement and continuity) can be much influenced, not only by the chosen moveout operator, but also by the employed apertures. We consider two, so-called, diffraction-stack moveouts, together with corresponding apertures, designed to enhance reflections and diffractions, respectively. The first moveout under consideration is the zero-offset (ZO), common-reflection-surface (CRS) diffraction moveout, that is obtained from the general ZO CRS moveout in the case that the target reflector reduces to a point. The second is the double-square-root (DSR) moveout, well established in time migration. To simplify the terminology, we shall refer to the ZO CRS diffraction moveout as the single-square-root (SSR) moveout. The SSR and DSR moveouts will be given specific apertures based on the Projected Fresnel Zone (PFZ), SSR with small apertures in midpoint, produced comparable results as the ones of conventional CRS with full-parameter reflection moveouts with reduced computational cost. In both situations, reflections are enhanced and diffractions attenuated. However, DSR with large midpoint apertures yield stacked sections in which diffractions are enhanced and reflections attenuated. The aperture size for optimal stacking is quantified by means of the PFZ that corresponds to the events (reflections or diffractions) under consideration. Synthetic and field data confirm a good potential of the proposed approach for image-quality improvement.

INTRODUCTION

In seismic processing, stacking is probably the tool of most widespread use. The reason is simple: Stacking takes advantage of the large redundancy of seismic data to "clean" the data, i.e., to significantly enhance the signal-to-noise ratio, as well as having events (say, reflections/diffractions) better suited for more reliable interpretation. Stacking operators are designed to enhance desirable events by constructive interference, while attenuating undesired events or noise by destructive interference.

Because of their robustness and simplicity, diffraction traveltimes occupy a prominent place as stacking operators, the best example being their role in Kirchhoff-type migration. A good reason for the great success of diffraction-stack traveltimes stems from Huygen's principle, in which the reflection response of a reflector can be thought as a superposition of the responses of point scatterers densely distributed on the reflector.

Good stacking depends on a number of factors, including (a) a stacking operator (moveout) that is able to accurately follow (approximate) desired events, (b) a coherence measure that is able to quantify how well the stacking operator approximates the desired events, (c) possible weights to improve the stacking and/or producing more meaningful amplitudes and (d) carefully chosen apertures that are able to focus stacking where only constructive interference takes place.

Here, we examine the influence of midpoint aperture under the use of two diffraction operators, namely (a) the ZO CRS diffraction moveout, referred throughout as the single-square-root (SSR) moveout and (b) the double-square-root (DSR) diffraction moveout. The SSR is a simplified version of the conventional ZO CRS moveout, that results when the target reflector reduces to a (diffraction) point. The DSR, of widespread use in time migration, is an exact expression of a point-diffraction response in a homogeneous medium. In fact, one can show that SSR is the second-order, Taylor-polynomial representation of the DSR.

In this work, we find that small apertures in midpoint produce enhanced reflections and attenuated diffractions. On the other hand, large apertures in midpoints produce enhanced diffractions and attenuated reflections. In the case of reflection enhancement, stacking results obtained using the SSR are comparable to the ones obtained (at a higher computational cost) by conventional, full-parameter CRS. However, use of the DSR moveout with large midpoint apertures, leads to significant enhancement of diffractions together with attenuation of reflections.

The aperture size for optimal stacking in both situations is quantified by means of the projected Fresnel Zone (PFZ) that corresponds to the events (reflections or diffractions) under consideration. Synthetic and field data confirm a good potential of the proposed approach.

SSR AND DSR MOVEOUTS

In the following, we introduce and briefly discuss the SSR and DSR moveouts. Our task is greatly facilitated by their widespread and routine use in seismic processing.

SSR moveout

As previously indicated, SSR is a particular case of the full CRS in the case that the target reflector reduces to a (diffraction) point. We recall (see, e.g., Jäger et al., 2001; Duvencq, 2004) that the CRS method is based on the generalized hyperbolic traveltime, which uses first and second derivatives with respect to midpoint and half-offset in the vicinity of a selected central or reference ray.

In the general case of a finite-offset central ray, the number of parameters of the CRS traveltime is five and fourteen for the 2D and 3D situations, respectively. Here we adopt the simpler case (of much more widespread use) in which the central ray is a ZO ray and also assuming non converted data and an isotropic medium, the number of CRS parameters reduces to, respectively, three and eight parameters for 2D and 3D datasets. The 3D ZO CRS hyperbolic traveltime reads

$$t_{CRS}(\mathbf{m}, \mathbf{h}) = \sqrt{[t_0 + \mathbf{a}^T(\mathbf{m} - \mathbf{m}_0)]^2 + (\mathbf{m} - \mathbf{m}_0)^T \mathbf{B}(\mathbf{m} - \mathbf{m}_0) + \mathbf{h}^T \mathbf{C} \mathbf{h}}, \quad (1)$$

where (\mathbf{m}, \mathbf{h}) denotes the midpoint and half-offset of a source receiver pair in the vicinity of the ZO central ray of coordinates $(\mathbf{m}_0, \mathbf{h} = \mathbf{0})$, with coefficients (CRS parameters) $\mathbf{a} = (a_i)$ (2×1 vector) and $\mathbf{B} = (B_{ij})$, $\mathbf{C} = (C_{ij})$ (2×2 symmetric matrices) given by

$$a_i = \frac{\partial t}{\partial m_i}, \quad B_{ij} = t_0 \frac{\partial^2 t}{\partial m_i \partial m_j} \quad \text{and} \quad C_{ij} = t_0 \frac{\partial^2 t}{\partial h_i \partial h_j}, \quad i, j = 1, 2, \quad (2)$$

all derivatives being evaluated at $\mathbf{m} = \mathbf{m}_0$ and $\mathbf{h} = \mathbf{0}$. As can be readily verified, the hyperbolic CRS traveltime of Equation (1) is directly obtained from its parabolic counterpart (namely a second-order Taylor polynomial of traveltime, instead of traveltime squared), by squaring both sides and retaining the terms up to second order only.

It is also well known that the parameter \mathbf{B} , in Equation (1), is by far the most unstable parameter, being attached to the so-called normal (N) wave and indirectly related to the curvature of the reflector at the normal-incident-point (NIP). This heavily contrasts with the good behavior exhibited by the remaining parameters, \mathbf{a} and \mathbf{C} , interpreted as slowness of the central ZO ray at its emergence point and the normal moveout (NMO) velocity, respectively. As the CRS parameter \mathbf{B} has the most unstable estimation, it would be attractive if, at least for initial estimations and lateral velocity variations, one could use a traveltime not dependent on that parameter.

Single square root (SSR) moveout

In order to avoid complications involved to estimate all CRS parameters, we propose to use a simplified version of Equation (1), in which we set $\mathbf{B} = \mathbf{C}$. The resulting expression, referred simply as single-square-root (SSR) moveout, is given by

$$t_{SSR}(\mathbf{m}, \mathbf{h}) = \sqrt{[t_0 + \mathbf{a}^T(\mathbf{m} - \mathbf{m}_0)]^2 + (\mathbf{m} - \mathbf{m}_0)^T \mathbf{C}(\mathbf{m} - \mathbf{m}_0) + \mathbf{h}^T \mathbf{C} \mathbf{h}}. \quad (3)$$

As well known (e.g., Duvencek, 2004), the above moveout readily follows from the full CRS counterpart in the case the target reflector reduces to a (diffraction) point. Substitution of full CRS moveout with the SSR moveout for stacking is not a new strategy (Garabito et al., 2001). In fact, the SSR moveout has a much longer tradition as a form of diffraction stack used in Kirchhoff migration. As shown below, in spite of the fact that the moveout (3) is naturally attached to diffractions, we find that such moveout can be very well suited to reflections, as long as proper apertures, in both midpoints and offsets, are chosen. More specifically, for reflection enhancement, a small aperture on midpoints should be used combined with a large aperture on offsets. The terms small and large refers to the convergence radius of the second-order approximation.

Double-square-root (DSR) moveout

Because of its Taylor expansion character, SSR fails to approximate the diffraction events when large apertures in midpoint and offset are considered. Trying to avoid such limitation, one can use smaller apertures in offset, which diminishes the benefits of redundancy. Moreover, in many cases, required near offsets are even not available in the dataset. As a remedy to overcome such drawbacks, we use a different diffraction traveltimes equation, also defined in terms of CRS parameters, namely the double-square-root (DSR). That is given by

$$t_{DSR}(\mathbf{m}, \mathbf{h}) = \frac{1}{2} \left[\sqrt{(t_0 + \mathbf{a}^T \Delta \mathbf{s})^2 + \Delta \mathbf{s}^T \mathbf{C} \Delta \mathbf{s}} + \sqrt{(t_0 + \mathbf{a}^T \Delta \mathbf{g})^2 + \Delta \mathbf{g}^T \mathbf{C} \Delta \mathbf{g}} \right], \quad (4)$$

where $\Delta \mathbf{s} = \mathbf{m} - \mathbf{h} - \mathbf{m}_0$ and $\Delta \mathbf{g} = \mathbf{m} + \mathbf{h} - \mathbf{m}_0$. The rule of thumb behind the use of DSR is that, as opposed to SSR, it provides an exact point-diffraction traveltimes in homogeneous media. As a consequence, at least for mild-to-moderate laterally velocity variations, DSR should be expected to well approximate diffractions in apertures comparable to the Fresnel zone associated with the measurement configuration. As depicted in Figures 1 and 2, that conjecture is confirmed in the simple situation of a point diffraction response within a vertically-inhomogeneous medium. The figures compare the SSR and DSR traveltimes the cases where the central midpoint is (a) vertically above the point diffractor and (b) laterally away (500 m to the left) from it. Based on the above considerations, our stacking strategy to enhance diffraction events is focused on the DSR moveout.

STACKING APERTURES

In the following, we examine the problem of choosing stacking apertures optimally designed for enhancing reflection or diffraction events. Our analysis uses the concept and properties of the Projected Fresnel Zone (PFZ), as introduced in Schleicher et al. (1997). We briefly explain the PFZ concept that refers to a given (central) source-receiver pair, (S, G) , as well as a target, subsurface reflector, Σ . Moreover, suppose that the pair, (S, G) , defines a unique reflection point, M_R , at Σ . The PFZ that corresponds to the above conditions represents the collection of points, (\bar{S}, \bar{G}) , in the neighborhood of (S, G) , for which

$$|t_{Ref}(\bar{S}, \bar{G}) - t_{Dif}(\bar{S}, M_R, \bar{G})| \leq \frac{w}{2}. \quad (5)$$

Here, $t_{Ref}(\bar{S}, \bar{G})$ is the reflection traveltimes of the reflection ray determined by (\bar{S}, \bar{G}) with respect to the target reflector and $t_{Dif}(\bar{S}, M_R, \bar{G})$ is the diffraction traveltimes, that corresponds to a diffraction point at M_R and source-receiver pair, (\bar{S}, \bar{G}) . Note that the reflection ray specified by (\bar{S}, \bar{G}) determines a reflection point, \bar{M}_R , that has a different location at Σ than the central reflection point, M_R , assumed as a diffraction

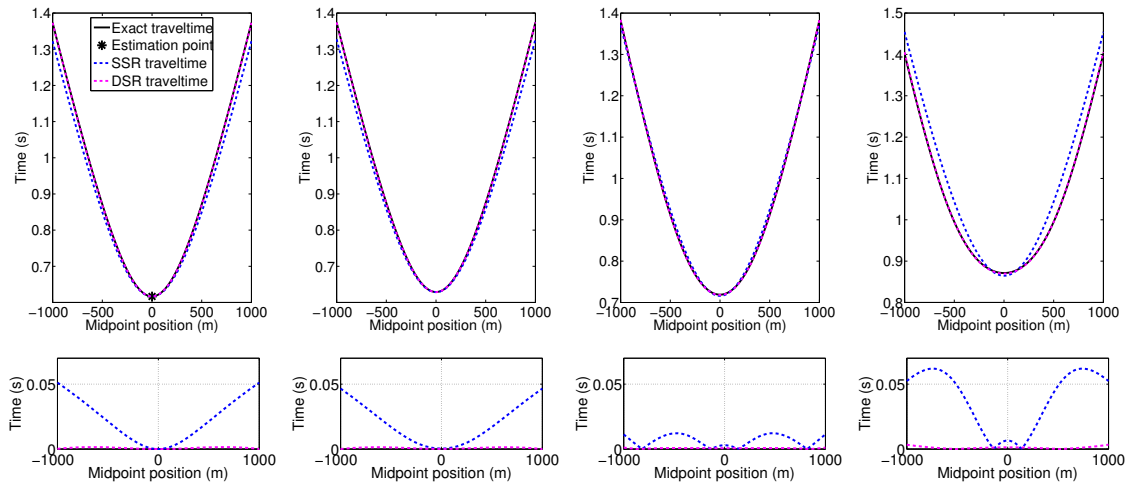


Figure 1: Comparison of the performances between the 2D SSR and DSR diffraction moveouts for the case of a point diffractor lying directly below the central point and at depth $500m$. The medium velocity is given by $v(z) = 1500 + 0.5z$, with velocity in km/s and depth coordinate in m . From left to right, the upper plots represent common-offset panels of offsets 0, 200, 600 and 1000 m. In the far left (ZO) panel, the fat black point represents the response of the diffractor point at the central point. Note that in this case, it lies at the apex of the travelttime curve. The lower plots represent the corresponding errors with the respect of the exact traveltimes.

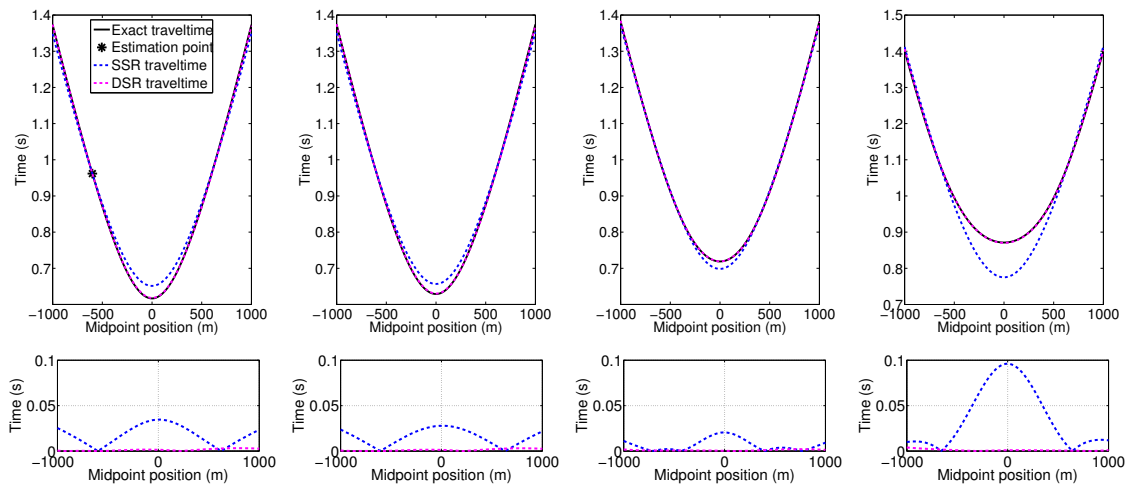


Figure 2: Comparison of the performances between the 2D SSR and DSR diffraction moveouts for the case of a point diffractor lying $500m$ to the left of the central point and at depth $500m$. The medium velocity is given by $v(z) = 1500 + 0.5z$, with velocity in km/s and depth coordinate in m . From left to right, the upper plots represent common-offset panels of offsets 0, 200, 600 and 1000 m. In the far left (ZO) panel, the fat black point represents the response of the diffractor point at the central point. Note that in this case, it lies at the apex of the travelttime curve. The lower plots represent the corresponding errors with the respect of the exact traveltimes.

point. All reflection and diffraction rays under consideration are assumed to have the same signature as the central ray, Finally, w is the pulse length.

One key observation is that, by its very definition, the size of the PFZ is small for reflections and large for diffractions in midpoint direction. As shown in Facciopieri et al. (2013) and Asgedom et al. (2013), the

use of large (midpoint) apertures in SSR can be very effective for imaging diffraction energy. However, the definition of what can be considered small and large should be better defined in order to achieve optimal results for diffraction or reflection enhancement. It should be noted that Asgedom et al. (2013) investigated CO-CRS and introduced a traveltime curve tailored for diffractions by generalizing a DSR type of moveout to a horizontally layered replacement medium. From this approach, proper bounds on the CRS parameters can be easily obtained, with the aperture size being directly related to the displacement of the apex of a given scatterer.

By considering midpoint and half-offset coordinates, the central and neighboring source-receiver pairs can be specified by $(\mathbf{m}_0, \mathbf{h}_0)$ and (\mathbf{m}, \mathbf{h}) , respectively. Moreover, we set $\mathbf{h}_0 = \mathbf{0}$, meaning that the central source-receiver pair is a ZO pair.

Our aim now is to express the PFZ inequality (5) in terms of the coefficients (CRS parameters) of the CRS, SSR and DSR traveltimes. For that purpose, it is convenient to introduce the parabolic version of these traveltimes, meaning the second-order Taylor polynomial approximations, denoted of the square-root expressions (1), (3) and (4), respectively. Denoted by t_{CRS}^{par} , t_{SSR}^{par} , and t_{DSR}^{par} , such parabolic traveltimes are easily seen to be given by

$$t_{CRS}^{par}(\mathbf{m}, \mathbf{h}) = t_0 + \mathbf{a}^T(\mathbf{m} - \mathbf{m}_0) + \frac{1}{2t_0} [(\mathbf{m} - \mathbf{m}_0)^T \mathbf{B}(\mathbf{m} - \mathbf{m}_0) + \mathbf{h}^T \mathbf{C} \mathbf{h}] . \quad (6)$$

and

$$t_{SSR}^{par}(\mathbf{m}, \mathbf{h}) = t_{DSR}^{par}(\mathbf{m}, \mathbf{h}) = t_0 + \mathbf{a}^T(\mathbf{m} - \mathbf{m}_0) + \frac{1}{2t_0} [(\mathbf{m} - \mathbf{m}_0)^T \mathbf{C}(\mathbf{m} - \mathbf{m}_0) + \mathbf{h}^T \mathbf{C} \mathbf{h}] . \quad (7)$$

Replacing the traveltimes t_{Ref} and t_{Dif} by their parabolic approximations (6) and (7) in the PFZ inequality (5) yields

$$|t_{Ref}(\mathbf{m}, \mathbf{h}) - t_{Dif}(\mathbf{m}, \mathbf{h})| = |(\mathbf{m} - \mathbf{m}_0)^T (\mathbf{B} - \mathbf{C})(\mathbf{m} - \mathbf{m}_0)| \leq wt_0 . \quad (8)$$

From basic results of Linear Algebra, we have that

$$|(\mathbf{m} - \mathbf{m}_0)^T (\mathbf{B} - \mathbf{C})(\mathbf{m} - \mathbf{m}_0)| \leq |\lambda| \|\mathbf{m} - \mathbf{m}_0\|^2 , \quad (9)$$

where

$$|\lambda| = \max\{|\lambda_1|, |\lambda_2|\} , \quad (10)$$

in which λ_1 and λ_2 are the eigenvalues of the 2×2 real matrix $(\mathbf{B} - \mathbf{C})$. As a consequence, the required inequality (8) is guaranteed whenever

$$\|\mathbf{m} - \mathbf{m}_0\| \leq \delta_{Ref}^{(m)} , \quad \text{with} \quad \delta_{Ref}^{(m)} = \sqrt{\frac{wt_0}{|\lambda|}} . \quad (11)$$

Equation (11) relates the midpoint aperture with the CRS matrices \mathbf{B} and \mathbf{C} . These apertures can be used, in principle, to stack reflections or diffractions. In many practical cases, the \mathbf{C} matrix will be of most significance. Gelius and Tygel (2015) have demonstrated how the eigenvalue of this matrix is related to the rms-velocity calculated along the corresponding normal ray used for time-to-depth mapping.

We finally note that we obtained no restriction for the half-offset aperture, $\delta_{Ref}^{(h)}$. Our proposal is, then, to consider

$$\delta_{Ref}^{(h)} = \delta_{CMP}^{(h)} , \quad (12)$$

which is the one used in conventional ZO CRS to obtain the matrix, \mathbf{C} using the common-midpoint (CMP).

Aperture for reflections

Actual use of the aperture expression (11) in practice can be greatly enhanced if the quantity, λ , is easily available in the seismic processing sequence. For that aim, we introduce the heuristic assumptions

$$|\lambda_B| \leq |\lambda_C| = \frac{4}{v_{NMO}^2} , \quad (13)$$

from which, substitution into the aperture equation (11) yields the sought-for aperture, denoted, δ_{Ref} with the expression

$$\delta_{Ref} = \frac{v_{NMO}}{2} \sqrt{\frac{wt_0}{2}}. \quad (14)$$

In Equations (13) and (14), v_{NMO} denotes the normal-moveout (NMO) velocity at the sample (m_0, t_0) .

Justification of equation (13) will now be given, for simplicity in the 2D situation only. For that aim, we recall the definitions of the ZO CRS (scalar) parameters B and C (Jäger et al., 2001)

$$B = \frac{2t_0}{v_0} \cos^2(\beta) K_N, \quad C = \frac{2t_0}{v_0} \cos^2(\beta) K_{NIP} = \frac{4}{v_{NMO}^2}. \quad (15)$$

In Equation (15), t_0 and v_0 represent, respectively, the traveltime along the (two-way) ZO central ray and the medium velocity at the emergence point of that ray at the surface. In the present 2D situation, the point where the ZO central ray emerges at the surface is specified by a scalar coordinate, m_0 . Next, β denotes the angle the central ray makes with the surface normal, also at m_0 . Finally, the quantities K_N and K_{NIP} , represent the wavefront curvatures of the N- and NIP-wavefronts, evaluated at m_0 . The N-wave starts as a wavefront that coincides with the reflector in the vicinity of the normal incident point (NIP), namely the point where the central ray hits the reflector. The NIP-wave starts as a point source at NIP.

In view of the above considerations, we see that, from the very definition of the (exploding reflector) N- and (point-source) NIP-waves, we can expect that, at least for not much pathological geologies, the absolute value of the wavefront curvature of the NIP-wave should be greater than the absolute value of curvature of its counterpart N-wave, namely, $|K_N| \leq |K_{NIP}|$, implying that $|B| \leq |C|$. In other words, the curvature of the reflection traveltime curve, B , is expected to satisfy $-|C| \leq B \leq |C|$. Jumping from 2D to 3D is not that trivial except from cases where the azimuthal variations are small and gentle. Leaving a more thorough investigation to further studies, the 2D heuristic considerations are assumed to here be valid in the 3D situation.

We observe that, once the apertures, $\delta_{Ref}^{(m)}$ and $\delta_{Ref}^{(h)}$ are defined, the estimation of \mathbf{a} and \mathbf{C} can be performed using Equation (3). The stacking is then performed with the same apertures used on the estimation of parameters. Figure 3 (left) shows the difference between the original PFZ and $\delta_{Ref}^{(m)}$ sizes.

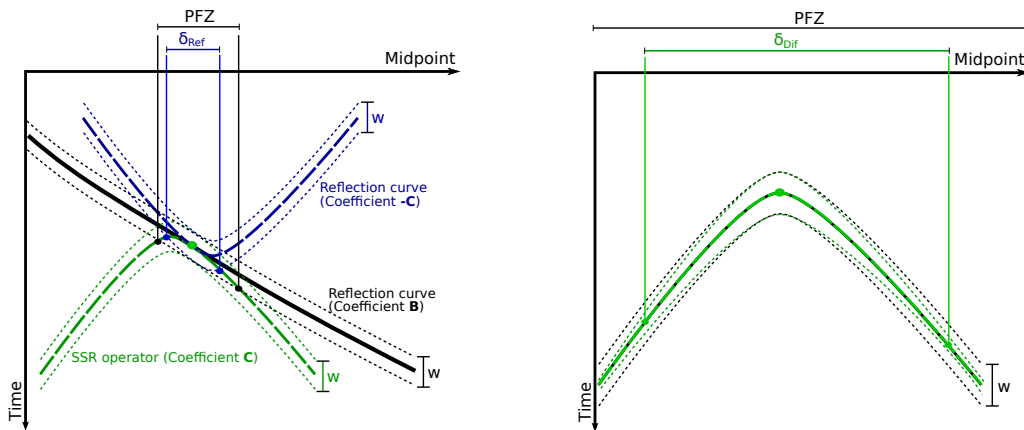


Figure 3: Left: PFZ for a ZO reflection event with pulse length w at a given point (m_0, t_0) , highlighted in green. Note how the midpoint aperture for the SSR moveout, $\delta_{Ref}^{(m)}$, well adjusts small region of the reflection event. Right: PFZ for a ZO diffraction event with pulse length w at a given point (m_0, t_0) , highlighted in green. Note that the aperture in midpoints for DSR, $\delta_{Dif}^{(m)}$, adjusts a much larger region of the diffraction event.

Aperture for diffractions

We now address the problem of finding a most adequate aperture for diffraction enhancement in the stacking process. In the same way as in our previous discussion on reflection enhancement, we base our discussion

on equations (5) and (8), taking into consideration that the reflection traveltime, t_{Ref} , is better approximated by a diffraction traveltime. Physically, this means that the target interface significantly shrinks (has a very large curvature), its shape being better approximated as a point rather than a reflector interface. In that situation, $t_{Ref} \approx t_{Dif}$, so that, theoretically, the midpoint aperture tends to infinity. Under these circumstances, our strategy is to take the largest possible midpoint aperture, as long as the stacking traveltime remains a reliable approximation of the traveltime of the observed event (see Figure 3 (right)). The above argument justifies the choice of the DSR moveout, as it provides a better approximation of diffraction traveltimes for large midpoints and also offsets.

To select optimal midpoint and half-offset apertures, $\delta_{Dif}^{(m)}$ and $\delta_{Dif}^{(h)}$ to enhance diffractions using the DSR moveout, we adopt the following strategy: For each sample, (\mathbf{m}_0, t_0) on which the stacking will be performed, we take, as before,

$$\delta_{Dif}^{(h)} = \delta_{CMP}^{(h)}, \quad (16)$$

namely, the aperture employed to estimate the matrix \mathbf{C} using the CMP configuration. For the midpoint aperture, $\delta_{Dif}^{(m)}$, we propose here the choice

$$\delta_{Dif}^{(m)} = \delta_{Dif}^{(h)} = \delta_{CMP}^{(h)}, \quad (17)$$

namely, we take equal apertures in midpoint and half-offset.

EXAMPLE: REAL MARINE DATA

The proposed approach was applied to a 2D marine real dataset acquired offshore in Brazil with 4ms of time sampling, 12.5 m between Common Midpoint (CMP) gathers with maximum fold of 60 traces. The pre-processing steps applied on this data set can be found in Facciopieri et al. (2013).

In order to demonstrate the effectiveness of the SSR estimation and stacking to enhance reflections, we processed the data by (a) conventional CRS, based on the CRS traveltime of three parameters, A , B and C of Equation (1) and (b) the alternative approach, which employs the SSR of two parameters, a and C , as given by Equation (3). In both situations, we assume that velocity analysis has been previously carried out. In this way, an estimation of NMO-velocities, v_{NMO} , and offset (CMP) apertures, $\delta_{CMP}^{(h)}$ are supposedly available. We also assume that the dominant frequency of the data, w , has been already estimated.

Under these circumstances, we perform, for both CRS and SSR situations, global estimation of parameters. The last step for our imaging is stacking and here the choice of aperture is crucial. In both cases, we used the apertures in midpoint and half-offset as prescribed by Equations (12) and (14).

Figure 4 compares three illustrative stacked traces under the use of CRS and SSR, respectively. The corresponding entire sections are displayed in Figure 5. The results are very similar, with the SSR stack slightly better, showing less high-frequency noise. However, since the proposed minimum aperture reduces the influence of parameter B one can state that if a larger aperture in midpoints were used, the resulting stacked section should be better.

Figure 6 shows a stacked section obtained with the CRS traveltime with the double of the minimum aperture used on the previous example. Note that the resolution was compromised and the reflectors heavily smoothed.

The results for diffraction enhancement using the proposed aperture in midpoint is shown on Figure 7 for SSR and DSR traveltimes. The apertures in offset direction for the SSR traveltime were three times smaller than the ones used with the DSR traveltime to ensure both traveltimes yield reliable approximations. Nevertheless, the DSR showed better separation of events and almost no residual reflections as expected, since it can use more traces to construct every sample on the stacked section. In order to illustrate the differences between SSR and DSR approximations, Figure 8 shows the stacked section obtained using SSR with the same apertures used to generate Figure 7 (right). In this case, SSR traveltime could not adjust to the diffractions on the longer offsets and produced blurred diffractions.

CONCLUSIONS

In the framework of CRS stacking, we propose an approach to reduce the number of parameters to be estimated in order to obtain a stacked section with reflections or diffractions. The diffraction SSR traveltime, which depends on less parameters than CRS, was investigated to stack reflection events. Stacked

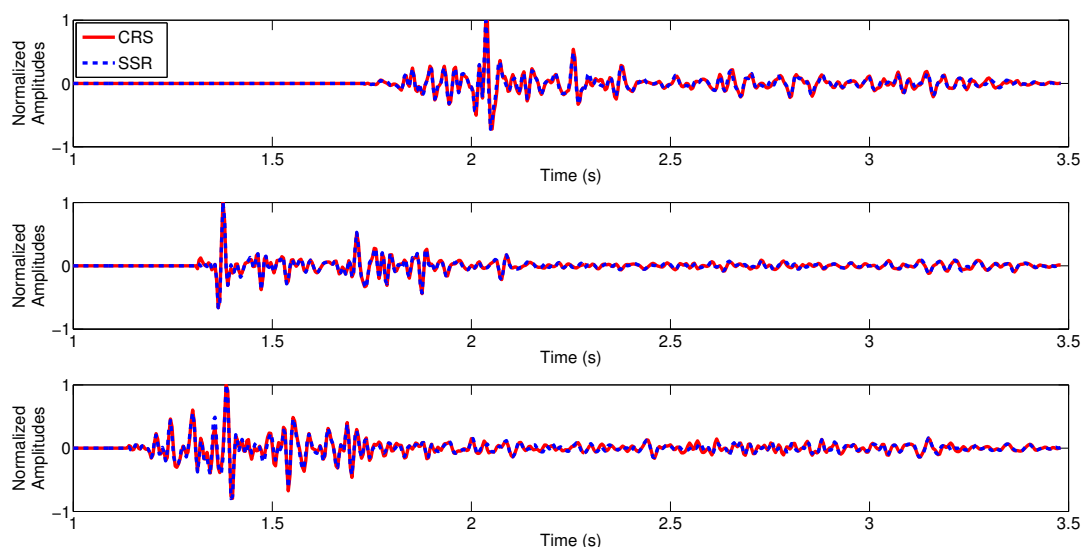


Figure 4: Comparison between three stacked traces, CMP's 750, 1000 and 1250, with minimum aperture in midpoint direction and large aperture in offset direction, obtained with the CRS traveltime, estimating a , B and C (solid red line) and with SSR traveltime, estimating a and C (dashed blue line).

sections obtained with SSR with varying apertures were tested and in the case of small apertures in midpoints, the results were slightly better and with lower computational cost to the ones obtained with the conventional CRS with full-parameter (designed for reflections). In both cases, reflections are enhanced and diffractions attenuated. Diffraction enhancement using SSR and DSR traveltimes were compared with varying apertures. The DSR with large midpoint and offset apertures produced cleaner stacked sections in which diffractions are enhanced and reflections attenuated. In addition, the quantification of small and large apertures was defined using the PFZ for optimal imaging of reflections and diffractions.

ACKNOWLEDGMENTS

J. Faccipieri, T. Coimbra and M. Tygel acknowledge support from the National Council for Scientific and Technological Development (CNPq-Brazil), the National Institute of Science and Technology of Petroleum Geophysics (ICTP-GP-Brazil) and the Center for Computational Engineering and Sciences (Fapesp/Cepid # 2013/08293-7-Brazil). All Authors acknowledge support of the sponsors of the Wave Inversion Technology (WIT) Consortium.

REFERENCES

- Asgedom, E. G., Gelius, L.-J., and Tygel, M. (2013). 2D common-offset traveltime based diffraction enhancement and imaging. *Geophysical Prospecting*, 61:1178–1193.
- Duveneck, E. (2004). 3D tomographic velocity model estimation with kinematic wavefield attributes. *Geophysical Prospecting*, 52(6):535–545.
- Faccipieri, J., Serrano, D., Gelius, L.-J., and Tygel, M. (2013). Recovering diffractions in crs stacked sections. *First Break*, 31:27–31.
- Garabito, G., Cruz, J. C., Hubral, P., and Costa, J. (2001). Common reflection surface stack: A new parameter search strategy by global optimization. In *SEG, Expanded Abstracts*, pages 2009–2012.
- Gelius, L.-J. and Tygel, M. (2015). Migration-velocity building in time and depth from 3D (2D) common-reflection-surface (CRS) stacking - theoretical framework. *Studia Geophysica et Geodaetica: Accepted for publication*.

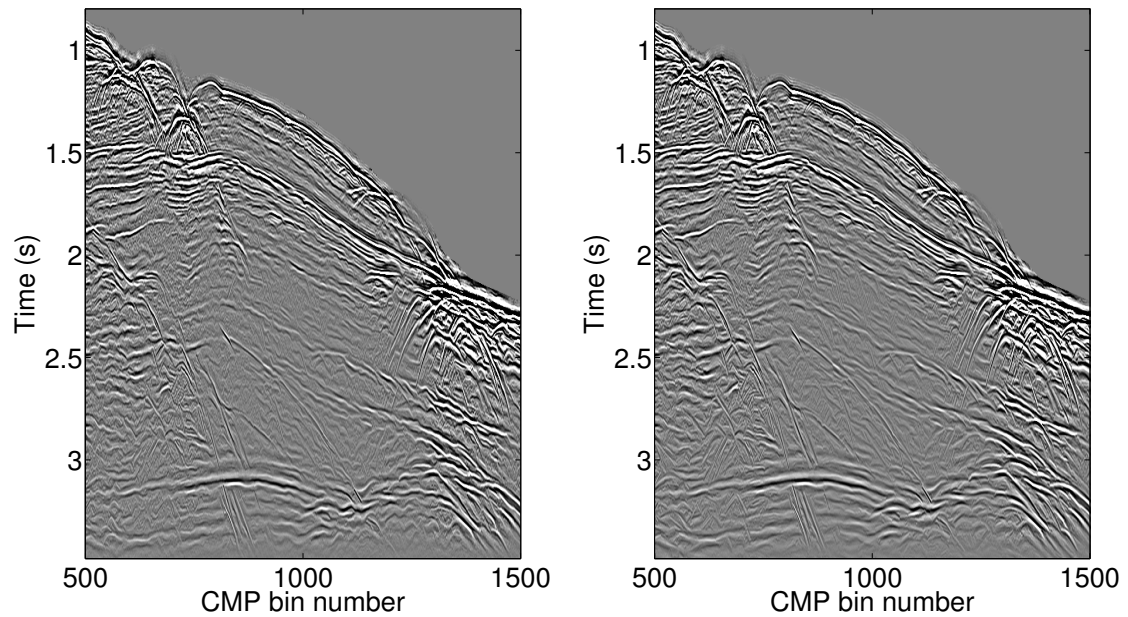


Figure 5: Reflection enhancement: Comparison between CRS (left) and SSR (right) stacked sections with minimum apertures in midpoints and large apertures in offset direction. Note that SSR showed less high-frequency noise.

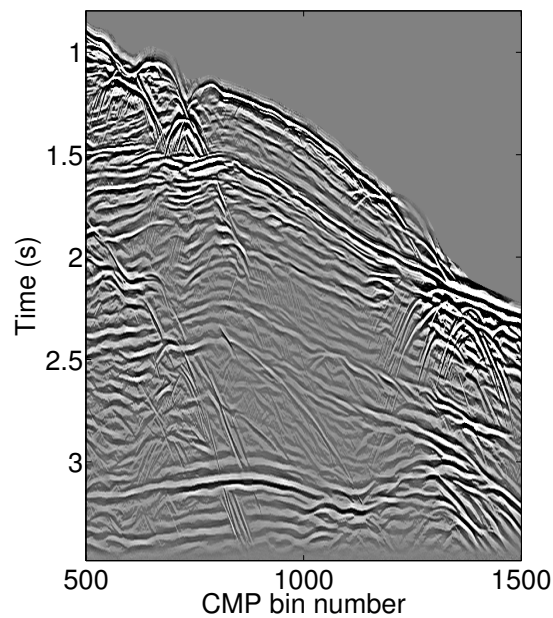


Figure 6: Reflection enhancement: Stacked section obtained with the CRS traveltimes using the double of the minimum aperture in midpoints. Note that the reflections were smoothed and resolution compromised.

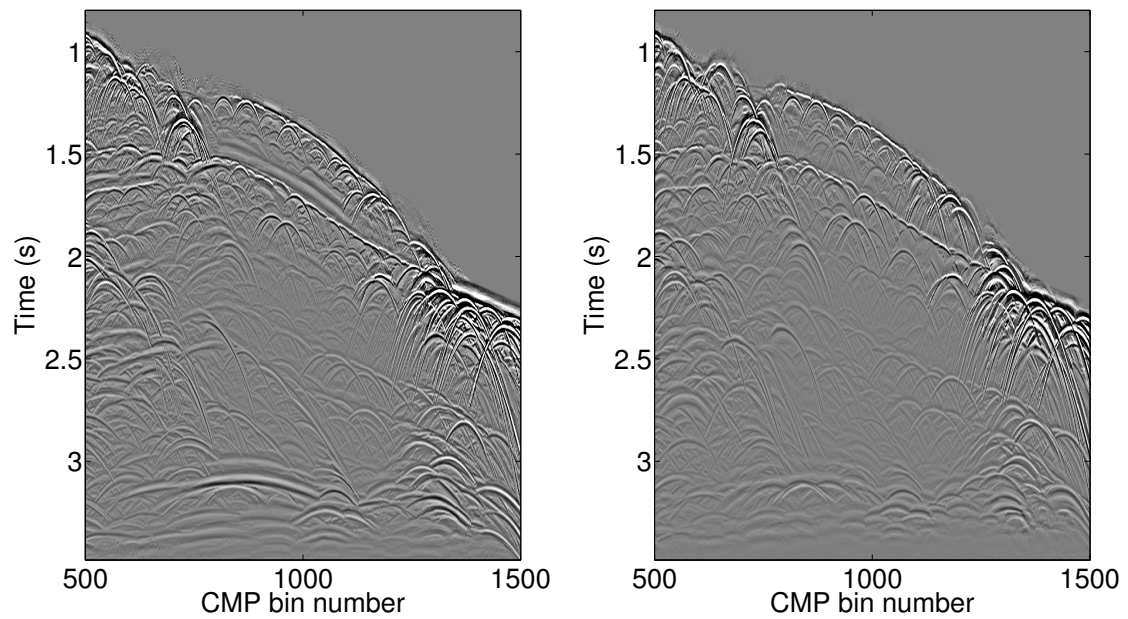


Figure 7: Diffraction enhancement: Comparison between SSR (left) and DSR (right) stacked sections with the same apertures in midpoint direction. Note that DSR obtained better separation of events and almost no residual reflections.

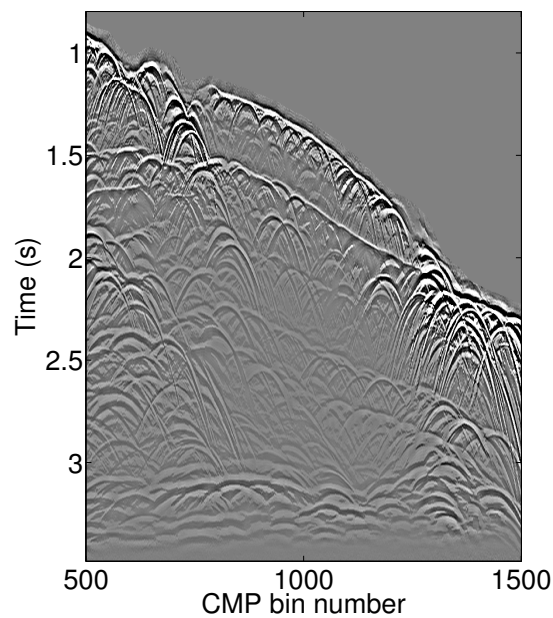


Figure 8: Diffraction enhancement: Stacked section obtained with the SSR traveltimes using the same apertures used to obtain Figure 7 (right). Note that the reflections were smoothed and resolution compromised.

Jäger, R., Mann, J., Höcht, G., and Hubral, P. (2001). Common-reflection-surface stack: Image and attributes. *Geophysics*, 66(1):97–109.

Schleicher, J., Hubral, P., Tygel, M., and Jaya, M. S. (1997). Minimum apertures and fresnel zones in migration and demigration. *Geophysics*, 62(1):183–194.